I J C T A, 10(5) 2017, pp. 679-690

Islanding Detection using DQ Transformation based PI Approach in Integrated Distributed Generation

Ch. Rami Reddy*, K. Harinadha Reddy*

Abstract: Although active islanding detection techniques have smaller non-detection zones than passive techniques, active methods could degrade the system power quality and are not as simple and easy to implement as passive methods. The islanding detection strategy, proposed in this paper, combines the advantages of both active and passive islanding detection methods. The distributed generation (DG) interface was designed so that the DG maintains stable operation while being grid connected and loses its stability once islanded. Thus, the over/under voltage and variation in the reactive power method be sufficient to detect islanding. The main advantage of the proposed technique is that it relies on a simple approach for islanding detection and has negligible non-detection zone. The proposed system was simulated on MATLAB/SIMULINK and simulation results are presented to highlight the effectiveness of the proposed technique.

Index Terms: Distributed Generation (DG), Inverter, Islanding, over/under voltage, Islanding Detection, Smart grid.

1. INTRODUCTION

Increasing distributed power generation sources, such as photovoltaic (PV), wind turbines, and fuel cells, are becoming commercially usable and part of daily life [1], [2]. Figure 1 presents the configuration of a typical distributed power generation system, which contains grid connected inverters to transmit electrical power to the grid [3]. Islanding is the phenomenon in which distributed generators and local loads are isolated from the grid but the system continues to operate. Unpredictable islanding of distributed power generation system may result in electrical damage to customer equipment, poor power quality, and even safety hazards for humans [4]. For these reasons, it is necessary to detect the islanding condition quickly and reliably. In addition, IEEE Std. 929 and IEEE Std. 1547 have specified some requirements of islanding detection tests, including the test circuit, the local loads selection method, and detailed procedures [5], [6]. For PV power generation systems, it is industry expectation to detect islanding within 2 s [7]. Many studies have been devoted to islanding detection methods and the main techniques can be classified into three categories: (1) passive methods; (2) active methods; and (3) communication-based methods. Passive methods usually monitor system parameters of grid-connected inverters such as voltage, frequency, phase, and harmonic distortion. When one or more of these parameters deviate from the permitted range, an islanding event is considered to have occurred. During practical applications of these detection techniques, the key point is how to set a proper threshold of monitoring parameters that are intended to identify islanding. In two basic islanding detection methods, namely over/under voltage protection and over/under frequency protection (OFP/UFP) [8], [9], the voltage threshold given in [7] is 85%–110% of normal value and the allowable frequency is set between 49.5 and 50.5 Hz for a 50-Hz system. Some other passive detection methods are available such as phase jump detection [10], voltage harmonic distortion measurement [11], [12] and voltage/power factor changes [13]. Numerical changes of system parameters due to islanding occurrence are related to the characteristics of the inverter and the local load. If the distributed generator and load power are closely matched, the deviations of monitored parameters are within the allowed ranges, and this will result in a non-detection zone (NDZ).

* ??

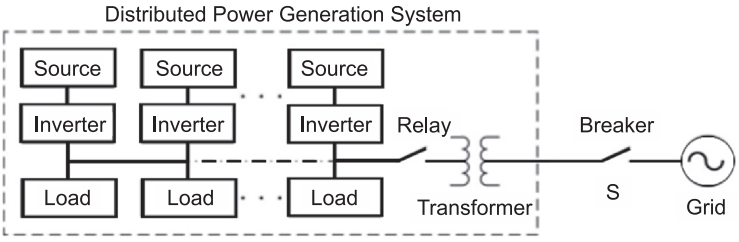

Figure 1: Block diagram of distributed power generation system

NDZ is the range of local conditions for which the islanding prevention method fails to detect the abnormal operation mode. Passive islanding detection methods suffer from large NDZs caused by the relatively large variation range of monitored parameters [14]. This is a major limitation of the passive detection method in practice. Active detection methods, on the other hand, force the islanded system to become unstable and monitor certain parameters to see if they exceed the normal range by introducing appropriate disturbances [15]–[17]. These active methods are capable of reducing NDZ compared with passive methods. Generally, active is landing detection methods include harmonic impedance measurement [18], active frequency drift or frequency bias [19], [20], Sandia frequency shift [21], slide-mode frequency shift [17], and Sandia voltage shift [22]. Furthermore, communication-based methods detect islanding applying the technology of power line carrier or introducing devices into the power and inverter systems. These methods can achieve islanding detection with no NDZ ,but the cost is much higher than the former ones [4]. Among published studies, islanding detection techniques based on reactive power variation (RPV) are more attractive because of the simplicity of implementation. In addition, RPV can eliminate the NDZ with proper design. Work proposed on [23] and [24], a straightforward RPV method was proposed. The inverter reactive output was changed periodically. The variation in amplitude was selected between +2.5% and −2.5% of rated active power. An improved reactive power drift method, referred to as the feedback approach, has been presented by Yiding Jin et. al., in [25], which controls the reactive power related to the system frequency. When an islanding event occurs, the frequency will shift away from the steady operating point and the controlled reactive power changes as a result, which will drive the frequency further away from the normal value. However, all of these studies have not shown detailed design methods of the reactive power value. The authors, [26]deduce there requirements for injected reactive power with the RPV detection method based on the characteristic analysis of system frequency variation caused by islanding. The time-domain formula for frequency variation under islanding operation mode was proposed using virtual impedance to substitute the intentionally injected reactive power. Nevertheless, the equivalence principle was lacking in detail. Huahan et. al., focus on the inverter output control and power sharing control which mostly belong to the primary control, especially for the droop-based control. Mostly, the decentralized control strategies are classified into four main categories more exactly [29].The researcher Rami reddy et. al., presented the power quality improvement in distributed generation [30].

2. SYSTEM UNDER STUDY

The system, shown in Figure 1, consists of a distribution network represented by a source behind impedance, a load represented in terms of R-L-C, and a 100 kW inverter based DG. The DG interface control model presented in was implemented and the DG is designed to operate as a constant power source by setting the controller's active and reactive reference values to fixed values. The reactive power reference value (Q_{ref}) is set to zero, thus simulating a unity power factor DG operation.

The DG interface has two sets of controllers: (1) For power regulation and (2) For current regulation as shown in Figure 2 The load is represented as a constant RLC load with an active and reactive power expressed as shown in equations (1) and (2)

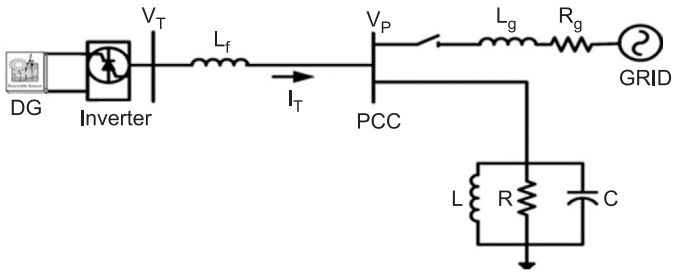

Figure 2: System under study

$$P = P_0 \left(\frac{v}{v_0} \right)^2 \tag{1}$$

$$Q = Q_0 \left(\frac{v}{v_0} \right)^2 \tag{2}$$

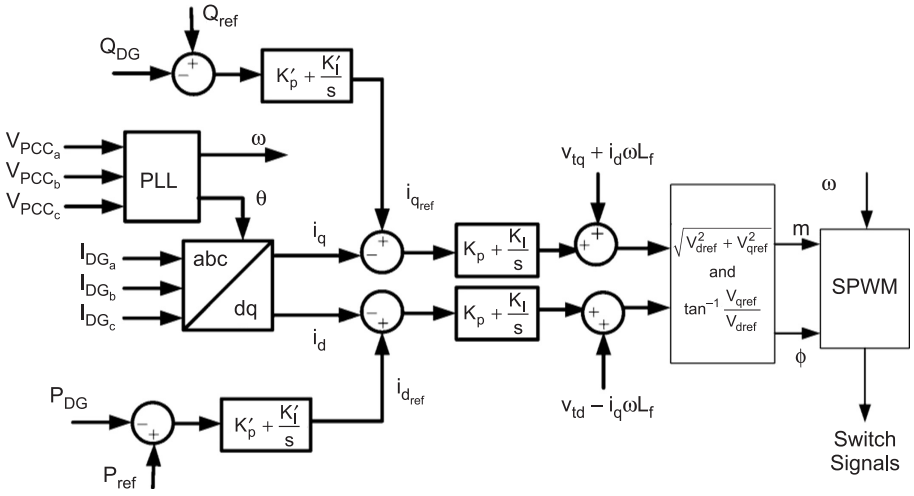

Figure 3: DG interface control for constant power operation

where V_0 represents the initial operating voltage and P_0 and Q_0 represent the active and reactive power corresponding to the initial operating voltage. The inductive and capacitive components of the load are modeled by using equation (2).The DG interface control variables are controlled by using the *d-q* synchronous reference frame. The instantaneous real and reactive power could be written in terms of the *d-q* axis components as follows [5], [8]

$$P = \frac{3}{2} V_{pd} I_{td} \tag{3}$$

$$Q = \frac{3}{2} V_{pd} I_{tq} \tag{4}$$

where V_{pd} is the *d*-axis component of the PCC voltage and is equivalent to the phase peak value at the PCC. The parameters I_{td} and i_t are the *d-q* components of the DG currents. Under balanced conditions, the *d-q* components of the voltage and current are constant quantities. The two current components are decoupled which facilitates independent regulation of the real and reactive power. The instantaneous voltages of the three phases could be expressed as follows

$$\frac{d}{dt} i_{tabc} = \frac{-R_f}{L_f} i_{tabc} + \frac{1}{L_f} (v_{tabc} - v_{pabc}) \tag{5}$$

where represents the DG current three-phase components and represent the filter resistance and inductance. Variables, and represent the DG terminal and PCC three phase voltages. By using Park's transformation can be transformed to the synchronously rotating reference frame as follows

$$\begin{bmatrix} i_{td} \\ i_{tq} \end{bmatrix} = \begin{bmatrix} -\frac{R_f}{L_f} & \omega \\ -\omega & -\frac{R_f}{L_f} \end{bmatrix} \begin{bmatrix} i_{td} \\ i_{tq} \end{bmatrix} + \frac{1}{L_f} \begin{bmatrix} v_{td} - v_{pd} \\ v_{tq} - v_{pq} \end{bmatrix} \tag{6}$$

The DG interface control is developed by using the set of equations as shown in Figure 3. The magnitude and angle of the modulating signal are calculated and are used to determine the inverter switching signals[28]. When the grid-connected inverter is under constant power control mode, the output active power and reactive power will remain unchanged in the islanding condition. Therefore, the following equations apply P = P, Q = Q.

The islanding frequency is given by

$$f^{I} = \frac{f}{4}\left[\sqrt{\left(\frac{\lambda_{PQ}}{Q_f}\right)^2 + 4} - \frac{\lambda_{PQ}}{Q_f}\right] \times \left[\sqrt{\left(\frac{Q_{Load}}{Q_f P_{Load}}\right)^2 + 4} - \frac{Q_{Load}}{Q_f P_{Load}}\right] \tag{7}$$

equation (7) shows that the islanding frequency is related to the characteristic parameters of the RLC load and inverter. The system frequency will change if the load power does not match the inverter output power. The islanding detection strategy, in which the frequency of the PCC voltage is monitored to determine an islanding occurrence if the value falls outside of the allowable range, is called the OFP/UFP method[27]

3. PRINCIPLE OF OVP/UVP AND (OFP/UFP)

Before going into the method description, an analysis related to the power balance of the system will be done in order to identify how monitored parameters can be affected when the energy flow is interrupted by the grid. Figure 4 shows the power balance of the system

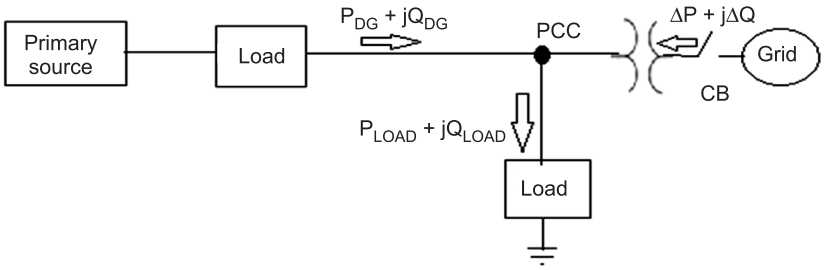

Figure 4: Power balance in a local load supplied both by the grid and a distributed generator

Equations (8) and (9) describe the power balance of the system.

$$P_{LOAD} = P_{DG} + \Delta P \tag{8}$$

$$Q_{LOAD} = Q_{DG} + QP \tag{9}$$

If $P_{LOAD} = P_{DG}$ and/or if $Q_{LOAD} = Q_{DG}$ there is not active or reactive power mismatch between the DG and the power grid. The behavior of the system when the grid is disconnected depends on the previous values of ΔP *y* ΔQ. It is worth to point out that the active power is directly proportional to the voltage. Therefore, if $\Delta P \neq 0$, the amplitude of the voltage will change. At first, when there is a disconnection of

the grid, the power consumed by the load is forced to be the same as the one generated by the DG, so that the voltage value in the grid changes to(10).

$$V^1 = \sqrt{\frac{P_{DG}}{P_{LOAD}}} + V \tag{10}$$

In the case of $P_{DG} > P_{LOAD}$, the voltage increases, otherwise it decreases, which might indicate whether the islanding conditions appears. Reactive power is a function of frequency and voltage width, so if $\Delta Q \neq 0$, the phase of the load voltage will present a sudden change and the control system will modify the signal frequency of the output current inverter to achieve $\Delta Q = 0$ (i.e. until it reaches the resonance frequency of the load). This change in the frequency may be detected to determine Islanding condition. The equation of reactive power in terms of frequency and voltage is presented by(11).

$$Q^1_{LOAD} = Q_{DG} = \left(\frac{1}{wl} - w^1 c\right) V^1 \tag{11}$$

Techniques of OVP/UVP and over/under frequency protection (OFP/UFP), allow the detection of islanding phenomenon through the measure of voltage and/or frequency at the Point of Common Coupling (PCC), and subsequent comparison with the limits set for proper operation. If the measured values are outside the established range, the inverter is stopped or disconnected. This method is not only a mechanism to detect islanding, it also protects the inverter.

The IEEE Std. 1547 and UL 1741 provide thresholds on the amount of acceptable voltage and frequency deviations. Thresholds on voltage deviations are in the range of 88% to 110% of the nominal voltage value .Any voltage deviation, resulting from an islanding condition, within these limits, would not be detected and the corresponding load would be considered in the NDZ. The load and DG P-V characteristics are analyzed to determine the amount of voltage deviation. Since the DG is designed to operate at a constant active power output, the DG power curve is represented with a horizontal line at 100 kW. For constant RLC loads, the active power is proportional to the square of the voltage.

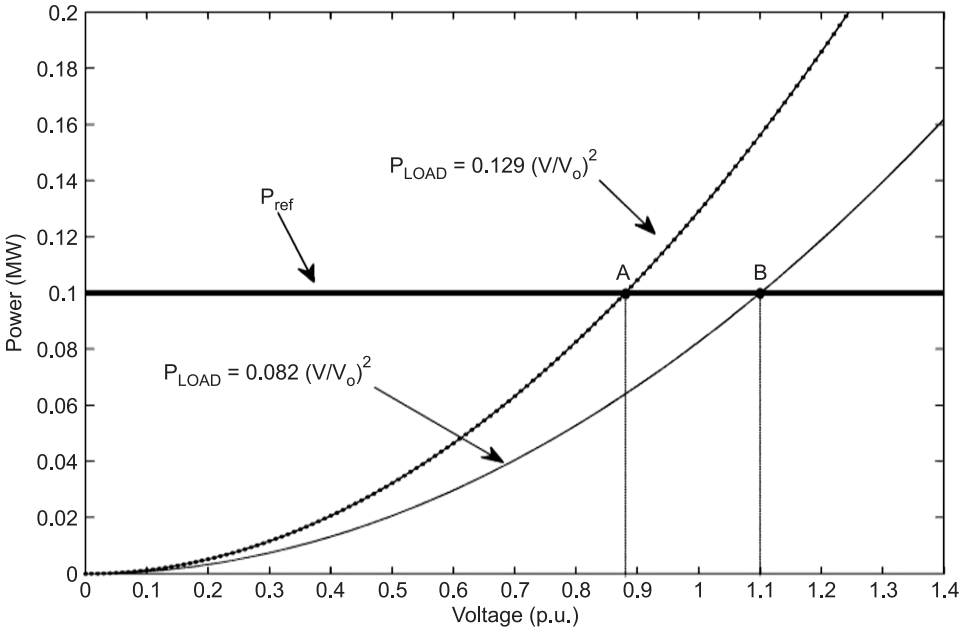

Figure 5: Power versus voltage characteristic for the DG and load with P_{ref} set to 100 kW

Figure 4 illustrates the P-V characteristic of the load and DG. The point at which the DG and load curve intersect is called the islanding operating point. It can be seen that for an islanded load of 129 kW,

the operating point "A" corresponds approximately to a voltage of 0.88 p.u. An 82-kW load corresponds approximately to a voltage of 1.1 p.u. The two loads represent the upper and lower active power limits. Any load with an active power curve between the two load curves presented in Figure 5 is considered within the NDZ. The results coincide with the active power mismatch presented in equation. It could be seen that one of the factors that results in the presence of a NDZ is the constant DG power curve. The active power mismatch of the NDZ is dependent on the DG P_{ref} setting. The DG reference power curve was modified and expressed as a function of its terminal voltage. The expression was formulated so that the DG delivers rated power at rated voltage. Figure 6 presents the power versus voltage curves for three loading conditions and the DG. The DG reference power is expressed in terms of voltage with the following equation

$$p_{\text{ref}} = 0.05\text{V} + 0.05 \tag{12}$$

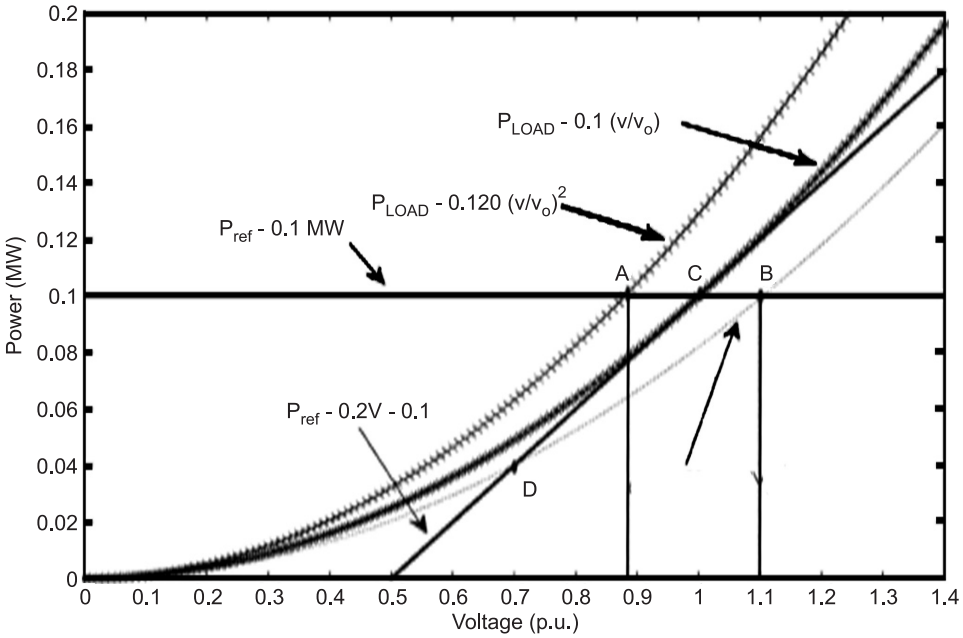

Figure 6: Power versus voltage characteristic for the DG and load with P_{ref} expressed as a function of the voltage with a positive slope.

The 100-kW load intersects the DG power curve at point "E" which corresponds to an active power of 100 kW and a voltage of 1 p.u. The 82-kW and 129-kW loads intersect the new DG curve at points "C" and "D". These two points correspond to voltage levels that are beyond the allowable voltage levels. Thus, these loading conditions will be easily detected using the over/ under voltage protection (OVP/UVP) method. The same two loading conditions were within the NDZ (points "A" and "B" in Figure 4) when the DG reference power curve was set to be fixed at 100 kW. Thus, the main idea behind the proposed technique is the reduction in the NDZ could be achieved by expressing P_{ref} as a function of voltage. Even though the NDZ has been reduced, we further explore different power voltage expressions to identify the mathematical expression that would result in the smallest NDZ. The reference power was further expressed as a function of voltage but with a negative slope the expression is

$$p_{\text{ref}} = -0.06\text{V} + 0.16 \tag{13}$$

The Figure 7 presents the power versus voltage curves for three loading conditions and the DG. Similarly, the 100-kW load intersects the DG power curve at point "M" which corresponds to an active power of 100 kW and a voltage of 1 p.u. The 82-kW and 129-kW loads intersect the new DG curve at points C^1 and D^1 and these two points correspond to voltage levels that are within the allowable voltage levels. Thus, these loading conditions will not be detected by using the OVP/UVP method and are within the NDZ. The same two loading conditions were at the border of the NDZ (points "A" and "B") when the DG reference power

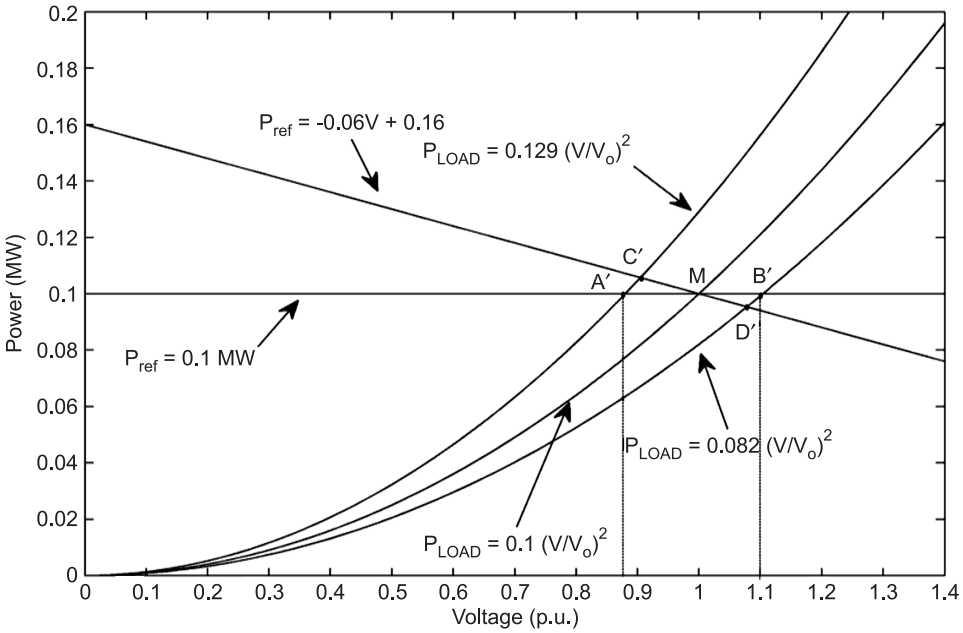

Figure 7: Power versus voltage characteristic for the DG and load with P_{ref} ex-pressed as a function of the voltage with a negative slop

curve was set to be fixed at 100 kW. Thus, using a power-voltage expression with a negative slope will lead to an increase in the NDZ. By comparing Figures 4 and 5, it can be seen that a P-V expression with a positive slope can reduce the NDZ of the OVP/UVP method. To further reduce the NDZ, the slope of the DG curve is increased until it reaches a point where the DG curve becomes a tangent to the 100 kW load curve. The DGP_{ref} could be expressed as follows:

$$p_{\text{ref}} = 0.2\text{V} - 0.1 \tag{14}$$

The technique does not require any additional control blocks. A simple and easy to implement islanding protection method, such as the OVP/UVP method, is implemented to detect the deviation in voltage once an islanding condition occurs. The analysis shows that by using the proposed P-V expression, the OVP/UVP will have negligible NDZ [28].

4. PERFORMANCE OF THE PROPOSED ISLANDING DETECTIONTECHNIQUE DURING AN ISLANDING CONDITION

The proposed islanding detection method was simulated on the system shown in Figure 2. An islanding condition is established by opening the utility breaker at $t = 0.1$s. The grid, DG and load voltages are shown in Figure 8. The Grid has the capacity to supply a load of 150 MVA, 11 KV at 50 Hz. The grid is supplying constant voltages when DG is connected. When grid is isolated from the DG the variations in load voltages are detected from the figure at $t = 0.1$ s and DG alone feeding power to load.

Table 1
Simulation parameters

Sl No	*Parameter name*	*Value*
1	Grid voltage	11 KV
2	Grid power, Frequency	150 MVA, 50 HZ
3	Transformer rating	11 KV/440 V, 250 MVA, 50 HZ
4	DG Rating	90 MVA, 440 V, 50 HZ
5	Non linear load	10 kW

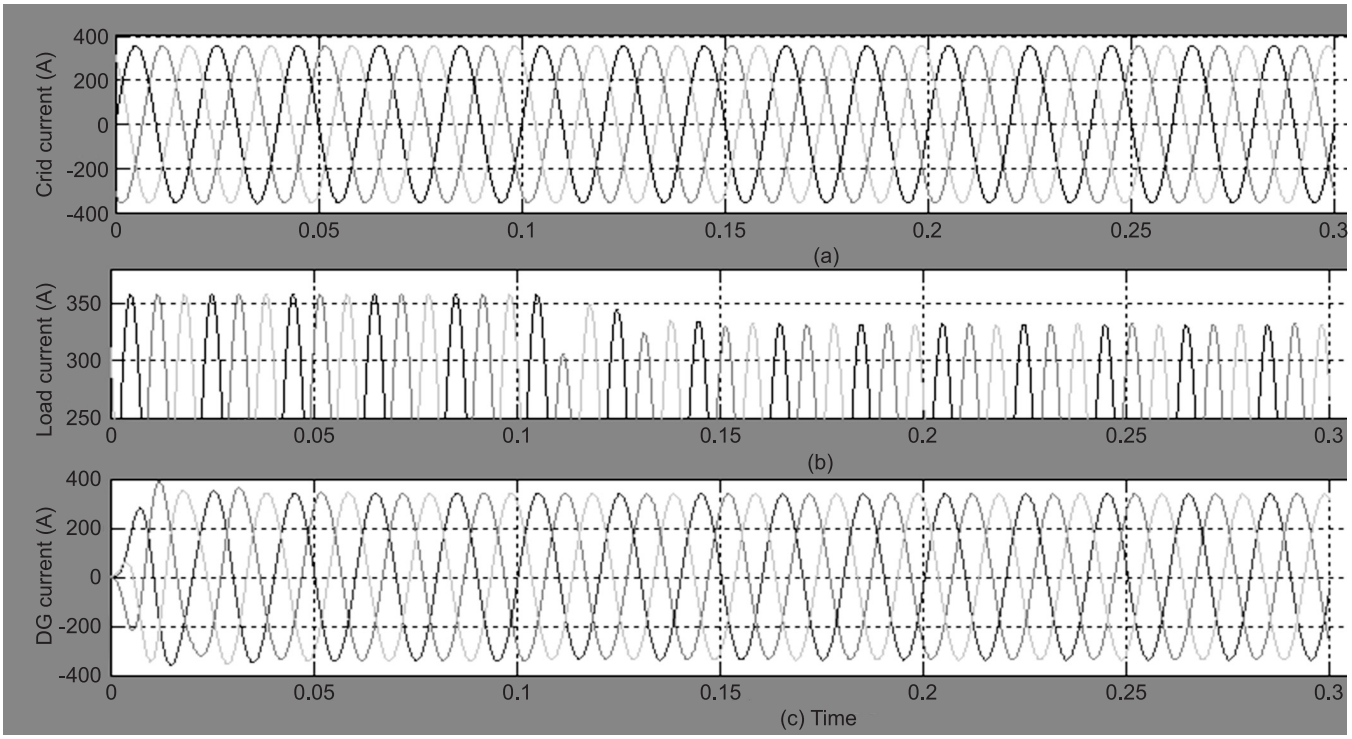

Figure 8: (a) Grid voltage, (b) load voltage and (c) DG voltage before and after islanding

The grid, DG and load currents are shown in Figure 8. The grid is supplying constant currents when DG is connected at t = 0.03s. Due to main circuit breaker opening at t = 0.1s island is created, and the grid currents are zero at t = 0.11s and DG alone feeding currents to load with less THD shown in Figure 8 (c).

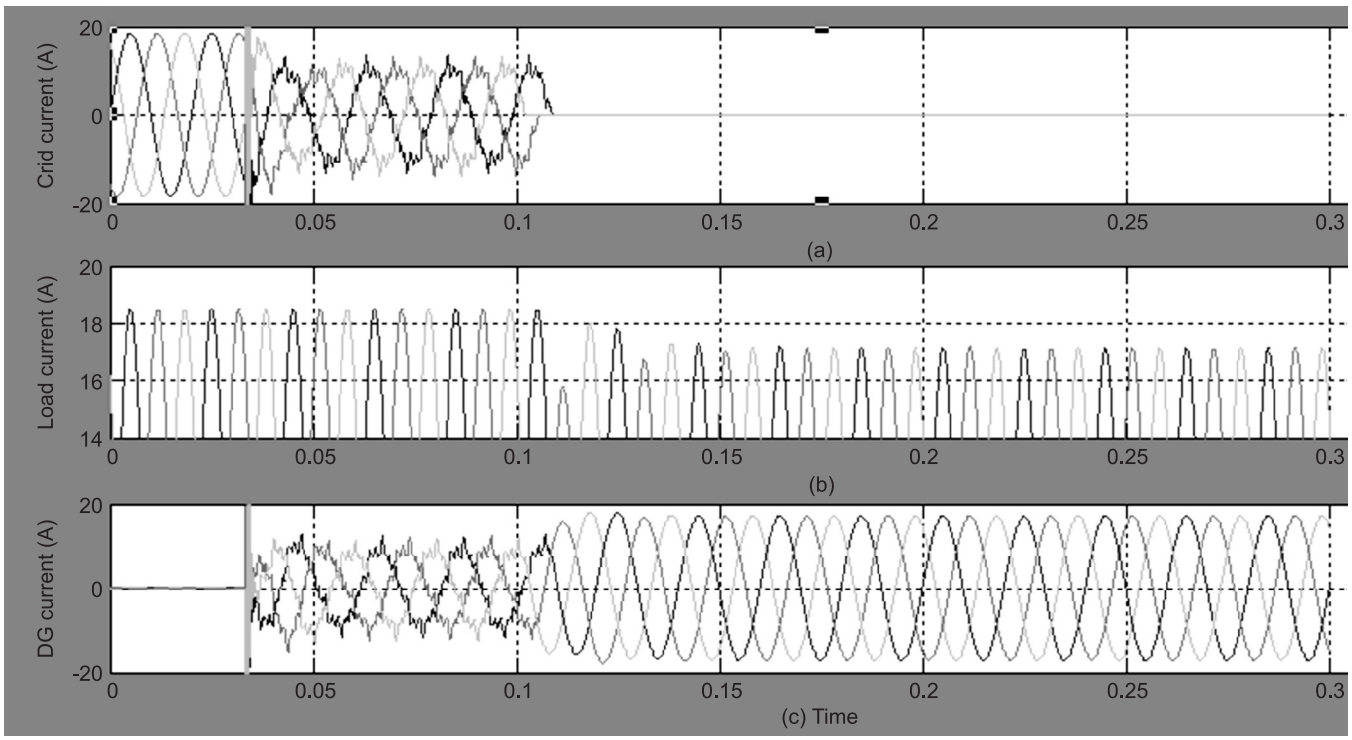

Figure 9: (a) Grid currents, (b) Load currents and (c) DG currents before and after islanding

Before the DG integration ,the grid is supplying 10 kW active power, at $t = 0.11$s the due to islanding condition the active power supplied by the grid is zero from Figure 10(a) and the DG is supplying required power to the load shown from Figure 11(a), this variation active power supplied by the load is detected by the Over voltage/under voltage relay placed at the point of common coupling

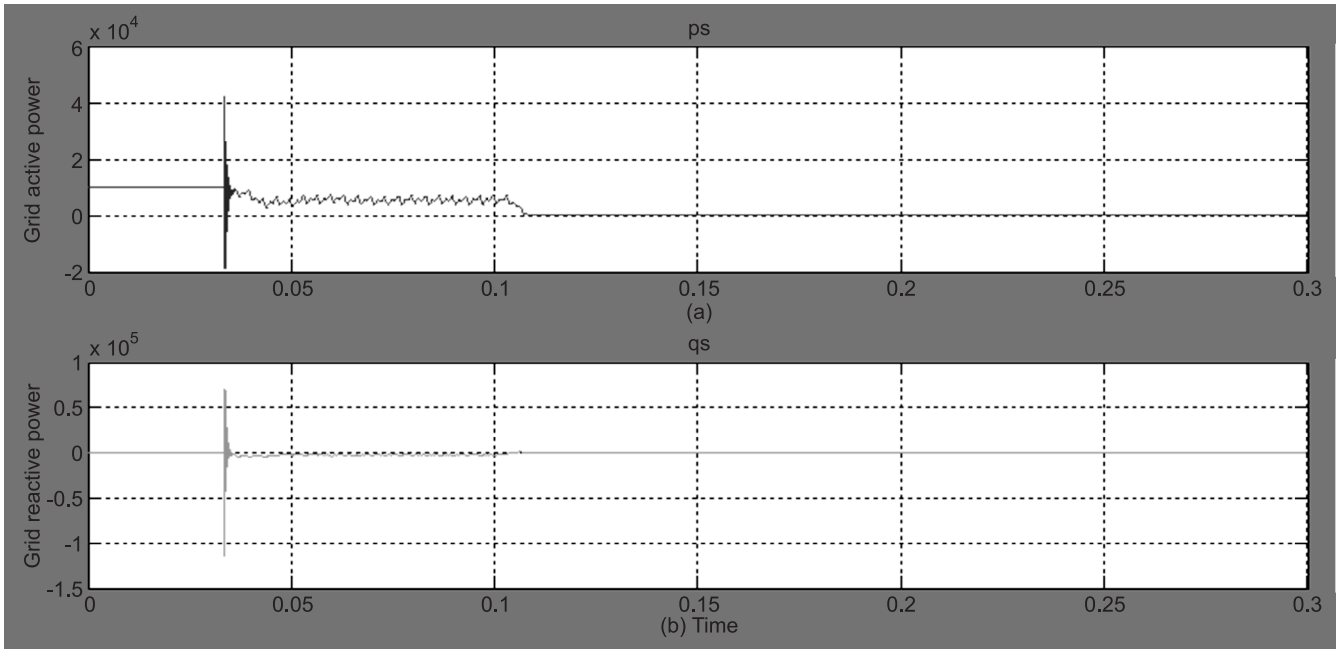

Figure 10: (a) Active power supplied by the Grid (b) Reactive power supplied by the Grid before and after islanding condition

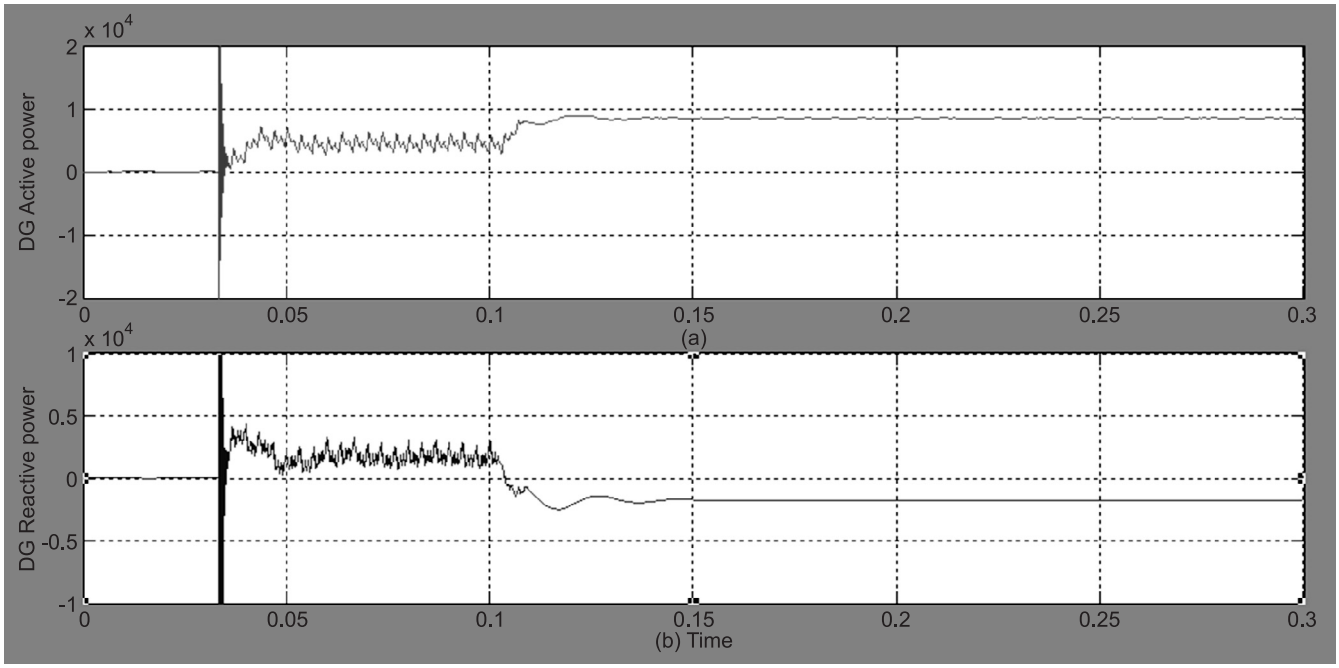

Figure 11: Simulation results of (a) Active power received by the Load (b) Reactive power received by the Load before and after islanding condition

The reactive power supplied by the DG before islanding condition occurred is observed from the Figure 11(b) is 200 VARS after islanding is supplying a reactive power of –200 VARS.the variation in this reactive power is detected by the over frequency/under frequency method of detecting the islanding condition.

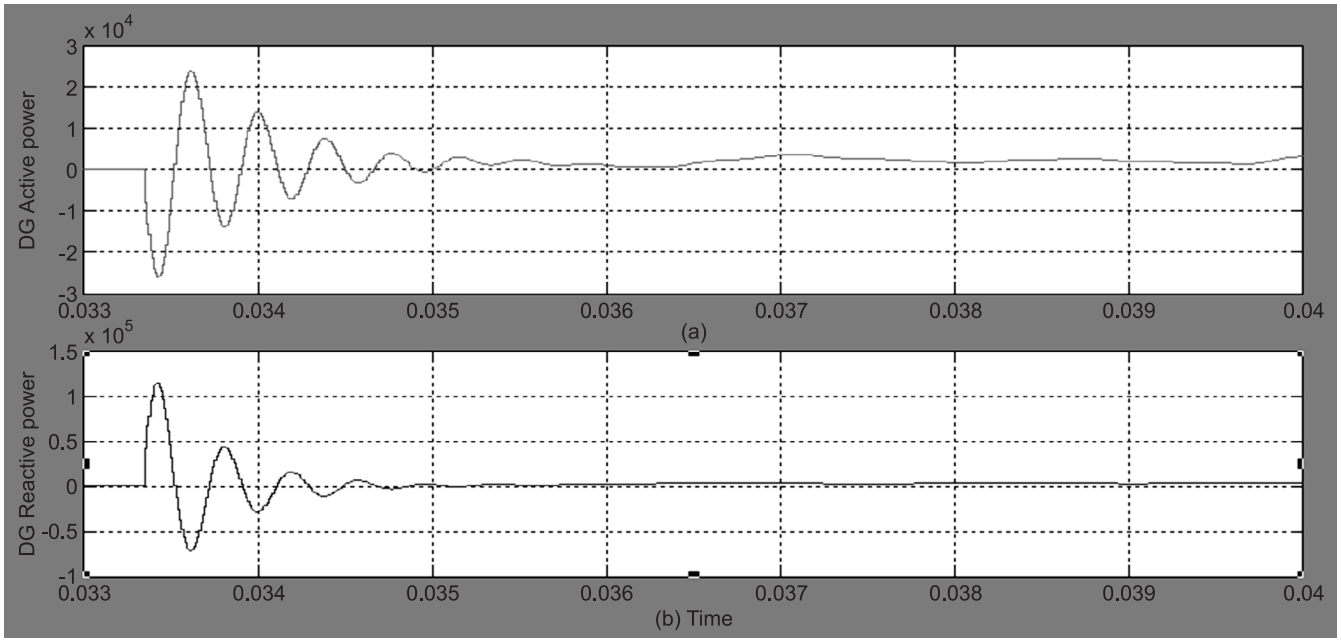

Figure 12. (a) DG active power settling time (b) DG Reactive power settling time when Grid connected to Islanded DG

5. CONCLUSION

This proposed method presents a new simple and easy to implement approach for islanding detection. The proposed idea relies on examining the voltage, current, active power, reactive power characteristics of the DG and load, and determining the best operating characteristics for the DG that will aid in islanding detection. The above characteristics of the DG was chosen so that the DG maintains stable operation while itis grid connected and loses its stability once islanded. The PCC voltage is monitored and the OVP/UVP method is used to disconnect the DG once it is islanded. The main advantages of the proposed technique include, unlike some of the previous active islanding detection methods, the proposed technique will not require additional controller blocks. Unlike the majority of passive methods, the proposed method has negligible NDZthe method is simple and easy to implement since it relies on utilizing the OVP/UVP and reactive power variations at PCC once it is islanded.

References

1. F. Blaabjerg, A. Consoli, J. A. Ferreira, and J. D. Van Wyk, "The future of electronic power processing and conversion," *IEEE Trans. Power Electron., Vol. 20, No. 3*, pp. 715-720, May 2005.
2. F. Blaabjerg, R. Teodorescu, M. Liserre, and A. V. Timbus, "Overview of control and grid synchronization for distributed power generation systems," *IEEE Trans. Ind. Electron., Vol. 53, No. 5*, pp. 1398-1409, Oct. 2006.
3. R. H. Lasseter, "Microgrids and distributed generation," *J. Energy Eng., Vol. 133, No. 3*, pp. 144-149, Sep. 2007.
4. M. Ropp and W. Bower, "Evaluation of islanding detection methods for photovoltaic utility interactive power systems" 2002.
5. IEEE Recommended Practice for Utility Interface of Photovoltaic (PV) Systems, *IEEE Standard 929-2000*, Apr. 2014.
6. IEEE Standard for Interconnecting Distributed Resources With Electric Power Systems, *IEEE Standard 1547-2003*, Jul. 2003.
7. Technical Requirements for Grid Connection of PV System, Chinese Standard GB19939-2005, Nov. 2005.
8. K. Tunlasakun, K. Kirtikara, S. Thepa, and V. Monyakul, "CPLD based Islanding detection forming rid connected inverter in renewable energy," *in Proc. IEEE TENCON Conf., Nov. 2004, Vol. 4*, pp. 175-178.

9. W. Freitas, W. Xu, C.M. Affonso, and Z. Huang, "Comparative analysis between ROCOF and vector surge relays for distributed generation applications," *IEEE Trans. Power Del., Vol. 20, No. 2, pt. 2*, pp. 1315-1324, Apr. 2005.
10. B. Singam and Y. Huil," Assessing SM Sand PJD scheme so anti-islanding with varying quality factor," in Proc. *IEEE Power Energy Conf., Nov.* pp. 196-201. March *2015,*
11. S. Jang and K. Kim, "An islanding detection method for distributed generations using voltage unbalance and total harmonic distortion of current," *IEEE Trans. Power Del., Vol. 19, No. 1*, pp. 745-752, Apr. 2004.
12. V. Menon and M.H. Nehrir, "A hybrid Islanding detection technique using voltage unbalance and frequency set point," *IEEE Trans. Power Syst., Vol. 22, No. 1*, pp. 442-448, Feb. 2007.
13. S.K. Salman, D.J. King, and G. Weller, "New loss of mains detection algorithm for embedded generation using rate of change of voltage and changes in power factors," *in Proc. Inst. Elect. Eng. Develop. Power Syst. Prot. Conf., 2001*, pp. 82-85.
14. H. H. Zeineldin, "A Q-f droop curve for facilitating islanding detection of inverter-based distributed generation," *IEEE Trans. Power Electron., Vol. 24, No. 3,* pp. 665-673, Mar. 2009.
15. X. Zhu, G. Shen, and D. Xu, "Evaluation of AFD islanding detection methods based on NDZs described in power mismatch space," in Proc. *IEEE Energy Convers. Congr. Expo., Sep., 2009,* pp. 2733-2739.
16. D. Velasco, C. Trujillo, G. Garcera, and E. Figueres, "An active antiislanding method based on phase-PLL perturbation," *IEEE Trans. Power Electron., Vol. 26, No. 4, pp.* 1056-1066, Apr. 2011.
17. K. Jae-Hyung, K. Jun-Gu, J. Young-Hyok, J. Yong-Chae, and W. ChungYuen, "An Islanding detection method for a grid-connected system based on the goertzel algorithm*," IEEE Trans. Power Electron., Vol. 26, No. 4*, pp. 1049-1055, Apr. 2011.
18. S. K. Chakravarthy, "Low frequency oscillations in a TCSC system," *IEEE Power Eng. Rev., Vol. 19, No. 4,* pp. 55-57, Apr. 1999.
19. H. Guo-Kiang, C. Chih-Chang, and C. Chern-Lin,"Automatic phase-shift method for islanding detection of grid-connected photovoltaic inverters," *IEEE Trans. Energy Convers., Vol. 18, No. 1*, pp. 169-173, Mar. 2003.
20. M. Roop, "Design issues for grid-connected photovoltaic system," *Ph.D. dissertation, Sch. of Electr. and Comput. Eng., Georgia Inst. of Technol., Atlanta, GA*, 1998.
21. M.E. Ropp, M. Begovic, A. Rohatgi, G. A. Kern, R. H. Bonn, and S. Gonzalez, "Determining the relative effectiveness of islanding detection methods using phase criteria and nondetection zones," *IEEE Trans. Energy Convers., Vol. 15, No. 3, pp*. 290-296, Sep. 2000.
22. W. Xiaoyu and W. Freitas, "Impact of positive-feedback anti-islanding method son small-signal stability of inverter-based distributed generation*," IEEE Trans. Energy Convers., Vol. 23, No. 3*, pp. 923-931, Sep. 2008.
23. J. B. Jeong, H. J. Kim, K. S. Ahn, and C. H. Kang, "A novel method for anti-islanding using reactive power," *in Proc. 27th INTELEC, 2005*, pp. 101-106.
24. J. B. Jeong, H. J. Kim, S. H. Back, and K. S. Ahn, "An improved method foranti islandingbyreactivepowercontrol,"*inPr oc.8thInt.Conf.Electr. Mach. Syst., Sep. 2005, Vol. 2,* pp. 965-970.
25. J. Yiding, S. Qiang, and L. Wenhua, "Anti-islanding protection for distributed generation systems based on reactive power drift," *in Proc .35th Ann. Conf. IEEE Ind. Electron., Nov. 2009, pp. 3970-3975*.
26. G.-H. Choe, H.-S. Kim, H.-G. Kim, Y.-H. Choi, and J.-C. Kim, "The characteristic analysis of grid frequency variation under islanding mode for utility interactive PV system with reactive power variation scheme for anti islanding," *in Proc. 37th IEEE Power Electron. Spec. Conf.,* Jun. 2006*, pp. 1-5.*
27. Jun Zhang, Dehong Xu, GuoqiaoShen,Ye Zhu, Ning He, and Jie Ma "An Improved Islanding Detection Method for a Grid-Connected Inverter With Intermittent Bilateral Reactive Power Variation" *IEEE transactions on power electronics, Vol. 28, No. 1,* pp.268-278 January 2013
28. Zeineldin, and James L. Kirtley A Simple Technique for Islanding Detection With Negligible Nondetection Zone H. H. *IEEE transactions on power delivery, Vol. 24, No. 2, April 2009*

29. Hua Han, Xiaochao Hou, Jian Yang, Jifa Wu, Mei Su, and Josep M. Guerrero "Review of Power Sharing Control Strategies for Islanding Operation of AC Microgrids*" IEEE transactions on smart grid, Vol. 7, No. 1, January 2016, pp 200-215.*

30. Ramireddychilakala, Srinusurtani, Anilkumar Obulasetty" Renewable Energy Sources Interconnection to the Grid at Distribution Level With Power-Quality Improvement Features" *International Journal of Engineering Research & Technology (IJERT) Vol. 2 Issue 12, December.*